0026-895X/07/7103-724–735$20.00
MOLECULAR PHARMACOLOGY
Copyright © 2007 The American Society for Pharmacology and Experimental Therapeutics
Mol Pharmacol 71:724–735, 2007

Vol. 71, No. 3
29223/3182485
Printed in U.S.A.

Identification of Leu276 of the $S1P_1$ Receptor and Phe263 of the $S1P_3$ Receptor in Interaction with Receptor Specific Agonists by Molecular Modeling, Site-Directed Mutagenesis, and Affinity Studies

Qiaolin Deng, Joseph A. Clemas, Gary Chrebet, Paul Fischer, Jeffrey J. Hale, Zhen Li, Sander G. Mills, James Bergstrom,[1] Suzanne Mandala, Ralph Mosley, and Stephen A. Parent

Departments of Molecular Systems (Q.D., R.M.), Immunology & Rheumatology (J.A.C., G.C., J.B., S.M. S.A.P.), Cardiovascular Diseases (P.F.), and Medicinal Chemistry (J.J.H., Z.L., S.G.M.), Merck Research Laboratories, Rahway, New Jersey

Received July 26, 2006; accepted December 4, 2006

ABSTRACT

Sphingosine-1-phosphate (S1P) receptor agonists are novel immunosuppressive agents. The selectivity of $S1P_1$ against $S1P_3$ is strongly correlated with lymphocyte sequestration and minimum acute toxicity and bradycardia. This study describes molecular modeling, site-directed mutagenesis, and affinity studies exploring the molecular basis for selectivity between $S1P_1$ and $S1P_3$ receptors. Computational models of human $S1P_1$ and $S1P_3$ receptors bound with two nonselective agonists or two $S1P_1$-selective agonists were developed based on the X-ray crystal structure of bovine rhodopsin. The models predict that $S1P_1$ Leu276 and $S1P_3$ Phe263 contribute to the $S1P_1$/$S1P_3$ selectivity of the two $S1P_1$-selective agonists. These residues were subjected to site-directed mutagenesis. The wild-type and mutant S1P receptors were expressed in Chinese hamster ovary cells and examined for their abilities to bind to and be activated by agonists in vitro. The results indicate that the mutations have minimal effects on the activities of the two nonselective agonists, although they have dramatic effects on the $S1P_1$-selective agonists. These studies provide a fundamental understanding of how these two receptor-selective agonists bind to the $S1P_1$ and $S1P_3$ receptors, which should aid development of more selective $S1P_1$ receptor agonists with immunosuppressive properties and improved safety profiles.

Sphingosine-1-phosphate (S1P) and lysophosphatidic acid (LPA) are important signaling molecules that activate a family of related G protein-coupled receptors (GPCRs) called endothelial differentiation gene (Edg) receptors (Chun et al., 2002). The receptors $S1P_1$ (Edg1), $S1P_2$ (Edg5), $S1P_3$ (Edg3), $S1P_4$ (Edg6), and $S1P_5$ (Edg8) bind S1P and regulate many cellular functions, including cell growth, proliferation, apoptosis, adhesion, and differentiation (Pyne and Pyne, 2000; Spiegel and Milstien, 2003). A role for S1P receptors in regulating immune function was discovered when the mechanism of FTY720 (Fig. 1) was elucidated. FTY720 is in clinical trials to prevent transplant rejection (Kiuchi et al., 2000) and is metabolized rapidly in the blood to the corresponding phosphate ester, FTY720-P (Fig. 1), which is a full agonist of $S1P_1$, $S1P_3$, $S1P_4$, and $S1P_5$ (Mandala et al., 2002). FTY720 causes immunosuppression by depleting peripheral blood lymphocytes, sequestering them in secondary lymphoid organs (Chiba et al., 1998) and preventing effector lymphocyte egress from draining lymph nodes to lymph and the blood compartment (Xie et al., 2003). FTY720 also has pleiotropic cardiovascular effects. In stable renal transplant patients, it causes a dose-dependent transient bradycardia (Budde et al., 2003) and, in anesthetized rats, either decreases or increases mean arterial pressure depending on the dose (Tawadrous et al., 2002).

S.A.P. and Q.D. contributed equally to this work.
[1] Current affiliation: Inexel Medical Strategy and Communication, Lawrenceville, New Jersey.

Article, publication date, and citation information can be found at http://molpharm.aspetjournals.org.
doi:10.1124/mol.106.029223.

ABBREVIATIONS: S1P, sphingosine-1-phosphate; LPA, lysophosphatidic acid; GPCR, G protein-coupled receptor; Edg, endothelial differentiation gene; TM, transmembrane helix; FTY720, 2-amino-2-[2-(4-octylphenyl)ethyl]propane-1,3-diol; FTY720-P, 2-amino-2-(hydroxymethyl)-4-(4-octylphenyl)butyl dihydrogen phosphate; compound A, 1-(3-methyl-4-{[4-phenyl-5-(trifluoromethyl)-2 thienyl]methoxy}benzyl)azetidine-3-carboxylic acid; compound B, 1-{4-[5-(4-isobutylphenyl)-1,2,4-oxadiazol-3-yl]benzyl}azetidine-3-carboxylic acid; CHO, Chinese hamster ovary; MMFF, Merck molecular force field; PCR, polymerase chain reaction; HT, hypoxanthine/thymidine; PDB, Protein Data Bank; TM, transmembrane; PBS, phosphate-buffered saline; GTPγS, guanosine 5′-*O*-(3-thio)triphosphate; FACS, fluorescence-activated cell sorting.

Studies on several S1P receptor agonists with varying degrees of selectivity (Hale et al., 2004a; Li et al., 2005) indicate that $S1P_1$ receptor agonism is strongly correlated with lymphocyte sequestration, whereas $S1P_3$ receptor agonism is associated with acute toxicity and bradycardia in rodents (Forrest et al., 2004; Sanna et al., 2004). For example, $S1P_1$-selective compounds A and B (Fig. 1) effectively alter lymphocyte trafficking and have much less potential to cause bradycardia and hypertension (Hale et al., 2004a; Li et al., 2005). The toxicity and bradycardia associated with the nonselective agonists S1P and FTY720-P were also abrogated in $S1P_3$ −/− mice confirming that $S1P_3$ agonism mediates these toxicities (Forrest et al., 2004; Sanna et al., 2004). These findings led us to study how $S1P_1$-selective agonists bind to $S1P_1$ and $S1P_3$.

GPCRs share a common 3D topology, consisting of seven *trans*-membrane helices (TMs) connected by three extracellular and three intracellular loops (van Rhee and Jacobson, 1996; Bosch et al., 2005; Fanelli and De Benedetti, 2005). S1P receptors belong to the largest subfamily A of GPCRs, which includes rhodopsin (for which high resolution X-ray crystal structures are available) (Palczewski et al., 2000; Teller et al., 2001; Okada et al., 2002; Edwards et al., 2004; Okada et al., 2004). Although the rhodopsin molecules are in the unactivated "dark state" in the structures, they provide attractive templates for homology modeling of family A GPCRs (Meng and Bourne, 2001; Archer et al., 2003; Bosch et al., 2005; Fanelli and De Benedetti, 2005).[2] Parrill and colleagues proposed homology models for $S1P_1$ and $S1P_4$ receptors bound to natural ligands and agonists based on a theoretically calculated rhodopsin model (Parrill et al., 2000; Inagaki et al., 2005; Jo et al., 2005). In their models, charged Arg and Glu residues at positions 3.28 and 3.29 on TM3 of $S1P_1$ and $S1P_4$ interact with the phosphate and ammonium moieties of the natural ligand S1P, respectively.

We describe molecular models of the $S1P_1$ and $S1P_3$ receptors bound to nonselective compounds S1P, FTY720-P, or $S1P_1$-selective compounds A or B based on the X-ray crystal structure of bovine rhodopsin (Palczewski et al., 2000). Energy-minimized conformations of agonists were docked into the proposed $S1P_1$ binding pocket. Two groups of residues were identified based on the nature of their interactions with the docked agonists. The first consists of Arg120(3.28) and Glu121(3.29), identified previously (Parrill et al., 2000; Inagaki et al., 2005; Jo et al., 2005). The second group consists of aromatic and hydrophobic residues on TM3, -5, and -6 that we propose form a hydrophobic binding pocket that interacts with the lipophilic chains of the agonists. One $S1P_1$ residue in this second group, Leu276(6.55), is not conserved in $S1P_3$, and our models predict that it contributes to the $S1P_1$ selectivity of compounds A and B. This $S1P_1$ residue and the corresponding Phe263 in $S1P_3$ were subjected to site-directed mutagenesis. The mutant and wild-type S1P receptors were expressed in Chinese hamster ovary (CHO) cells and examined for their abilities to bind to and be activated by agonists in vitro. Results from these experiments confirmed the predictions of our computational models and begin to provide an understanding of how compounds A and B bind $S1P_1$ selectively.

Materials and Methods

Sequence Alignment of S1P Receptors with Bovine Rhodopsin. The nomenclature proposed by van Rhee and Jacobson (1996) is used to describe the amino acid residues in the S1P receptors. Each residue is represented in two parts. The first part consists of the name and sequential number of an amino acid in a given S1P receptor sequence and is followed by a parenthesis with the second part, which is the index number defined by Ballesteros and Weinstein (1995). In the Ballesteros-Weinstein system, each residue identifier begins with the TM number (e.g., 3 for TM3) followed by the position in the helix relative to the most highly conserved residue that is assigned number 50. For example, the charged residue pair in TM3 is represented as 3.28 and 3.29 [i.e., Arg120(3.28) and Glu121(3.29) in $S1P_1$ and Arg114(3.28) and Glu115(3.29) in $S1P_3$].

Multiple sequence alignments of bovine rhodopsin, five human S1P receptors, three closely related human LPA receptors, and some selected GPCR subfamily A sequences were generated with the program ClustalW (Thompson et al., 1994). After computational alignment, manual adjustments were made to eliminate gaps in the TM regions.

Three-Dimensional Modeling of the $S1P_1$ Receptor. The homology model of $S1P_1$ was generated with the program Quanta/Modeler (Accelrys Software Inc., San Diego, CA) based on the X-ray crystal structure of bovine rhodopsin [Protein Data Bank (PDB) entry 1F88] (Palczewski et al., 2000). The amino-terminal 41 resi-

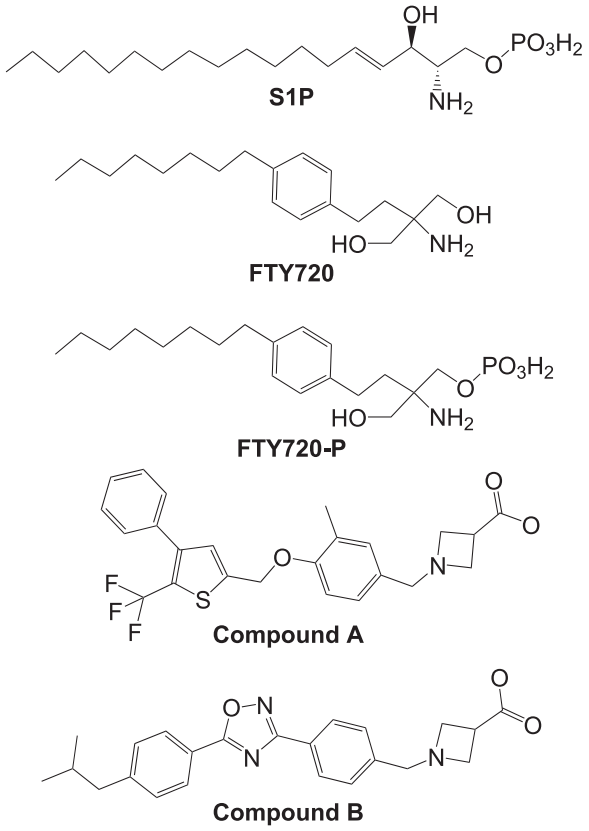

Fig. 1. The chemical structures of S1P, FTY720, FTY720-P, and compounds A and B.

[2] After the manuscript for this article was submitted, we noted the recent release of X-ray crystal structures of activated forms of rhodopsin, including bathorhodopsin (PDB entry 2G87) (Nakamichi and Okada, 2006a), lumirhodopsin (PDB entry 2HPY) (Nakamichi and Okada, 2006b), and a photoactivated deprotonated intermediate of rhodopsin (PDB entry 2I37) (Salom et al., 2006). Given the high structural similarities between bovine rhodopsin in the dark state and the activated forms, the use of the dark state rhodopsin (PDB entry 1F88) as a modeling template would seem to be a reasonable starting point for homology modeling of family A GPCRs bound to agonists and antagonists.

dues and carboxyl-terminal 51 residues of rhodopsin were excluded because of the lack of available template for these regions. The homology model was further refined using the Molecular Mechanics and Molecular Dynamics optimization to release the strain. The quality of the homology model was checked by Protein Health in Quanta (Accelrys Software Inc.). The $S1P_3$ homology model was constructed in a similar fashion. Because $S1P_1$ and $S1P_3$ receptors share high sequence identity and similarity, and the models were constructed using the same rhodopsin template, the models have very similar topologies with a root-mean-square deviation less than 1 Å for the receptor backbones. To minimize potential uncertainties introduced in modeling the flexible amino acid side chain structures, the $S1P_1$ homology model was used to dock agonists. The $S1P_3$ receptor was modeled based on the $S1P_1$ homology model by mutating the nonconserved residues. This minimizes potential artifacts from the homology modeling but retains the appropriate level of detail needed to select residues of interest identified through the docking studies.

Agonist Docking in the $S1P_1$ Receptor. The *S*-enantiomer of FTY720-P is its most potent enantiomer (Hale et al., 2004b) and was initially used in docking experiments because the affinities of the S1P enantiomers were unknown when these experiments were initiated. One hundred FTY720-P conformations were generated using our implementation of the distance geometry approach, which incorporates the theory and algorithm as described previously (Crippen and Havel, 1988). The conformer set was energy minimized using a distance-dependent dielectric of $2r$ with the MMFFs force field (Halgren, 1996). Manual docking placed the anionic phosphate and the positively charged ammonium of groups of FTY720-P close to the Arg120(3.28) and Glu121(3.29) on TM3. This docking placed the lipophilic chain of FTY720-P in a location similar to retinal in the rhodopsin-retinal complex. Because S1P and rhodopsin belong to GPCR subfamily A and the S1P receptor models were generated from and are similar to the rhodopsin crystal structure, the models place the lipophilic chains of FTY720-P in a hydrophobic pocket that is similar to that occupied by retinal between TM3, -5, -6, and -7. Ligand binding pockets lie between TM3, -5, -6, and -7 in many GPCRs, and this is considered a common feature for family A GPCRs (Bondensgaard et al., 2004). Docking models of the $S1P_1$ receptor with FTY720-P were obtained in a stepwise fashion to obtain the best docking pose and to minimize potential biases introduced by the initially manual docking of FTY720-P in the $S1P_1$ model. First, the hundred conformers of FTY720-P were docked into the putative binding pocket with their lipophilic chain superimposed onto the retinal structure by SQ calculations (Miller et al., 1999). The receptor complexes were energy optimized by MMFFs force field with the agonists fully optimized inside the binding pocket, which allowed some degree of flexibility. The side chains of residues with any atom located within 5 Å of the agonists were fully minimized in conjunction with the agonists. Residues falling within 5 to 10 Å of the agonists were included in the calculations as rigid elements, and the residues beyond a 10-Å cutoff from the agonist were ignored in the calculations. The total energy of the complex, the individual energies of the agonist and the receptor, and the interaction energy between the agonist and the receptor were calculated. The best docking mode was determined by selecting those poses with the most stabilizing interaction energy and minimal amount of strain on the agonist and by visual inspection of the interactions. This receptor-agonist model was used as a second template to superpose another hundred conformers, followed by the same procedure of energy optimization of complexes. The cycles continued until the docking pose could not be improved energetically. The docking models of $S1P_1$ receptor with S1P, compounds A and B, were derived from the final docking model of $S1P_1$ receptor with FTY720-P, through similar cycles of conformational searches and energy minimizations, superposition onto the template, energy optimizations of complexes, and determinations of best docking poses by energy and visual check of interactions. Other docking programs, such as ICM (Molsoft LLC, San Diego, CA), were used to generate FTY720-P docking poses in the $S1P_1$ receptor but did not generate more energetically favorable or new models.

Synthesis. The syntheses of compounds A and B have been described previously (Hale et al., 2004a; Li et al., 2005). All compounds were characterized by ^{1}H NMR, mass spectrometry, and high-performance liquid chromatography and were judged to be >95% pure.

Cloning the Human $S1P_1$ and $S1P_3$ Receptors into Expression Plasmids. An N-terminal Flag-tagged human $S1P_3$ receptor sequence was amplified from an expression vector provided by Kevin Lynch (University of Virginia, Charlottesville, VA) by PCR amplification using the primer set SAP470 (5′-GAATTCGCCACCATGGATTACAAGGATGACG-3′) and SAP471 (5′-GCGGCCGCTCAGTTGCAGAAGATCCCATTC-3′), which introduced a Kozak sequence, as well as EcoRI and NotI sites at the 5′ and 3′ termini, respectively. The accession number of the sequence of the human $S1P_3$ in this study is X83864, and the N-terminal Flag sequence (amino acids MDYKDDDDKSPGGS) replaces the initiator methionine codon of the human $S1P_3$ sequence. The PCR product was cloned into pCR4.0-TOPO (Invitrogen, Carlsbad, CA) and confirmed by DNA sequence analysis. The resulting plasmid, pJAC145, was digested with EcoRI and NotI, and the $S1P_3$ fragment was subcloned into compatible sites of pBluescript-KS II+ (Stratagene, La Jolla, CA) and the mammalian expression vector pCDEF3neo (Goldman et al., 1996), which contains the human EF-1a promoter. The resulting plasmids, pJAC149 and pJAC147-9, were confirmed by DNA sequence analysis.

An N-terminal Flag-tagged human $S1P_1$ receptor sequence was cloned from an expression plasmid provided by Kevin Lynch by PCR amplification using the primer set SAP468 (5′-GGATCCGCCACCATGGACTACAAGGACGACG-3′) and SAP469 (5′-GCGGCCGCCTAGGAAGAAGAGTTGACGTTTC-3′), which introduced a Kozak sequence as well as BamHI and NotI sites at the 5′ and 3′ termini, respectively. The accession number of the sequence of the human $S1P_1$ in this study is AF233365, and the N-terminal Flag sequence (amino acids MDYKDDDDKLEL) replaces the initiator methionine codon of the human $S1P_1$ sequence. The PCR product was cloned into pCR4.0-TOPO and confirmed by DNA sequence analysis. The resulting plasmid, pGC106-26, was digested with BamHI and NotI, and the $S1P_1$ fragment was subcloned into compatible sites of pBluescript-KS II+ and the mammalian expression vector pCDEF3neo (Goldman et al., 1996) to yield pGC109 and pGC108-C2, respectively. The sequences of the inserts in these plasmids were confirmed by DNA sequence analysis.

Site-Directed Mutagenesis of $S1P_1$ and $S1P_3$ Receptors. The $S1P_1$ Leu276Phe and $S1P_3$ Phe263Leu mutations were created in pGC109 and pJAC149, respectively, using the Transformer site-directed mutagenesis kit (Clontech, Mountain View, CA) and the manufacturer's recommended protocols. The mutagenic and selection primers and restriction enzyme used to generate the $S1P_1$ mutation were SAP486 (5′-phosphate-CTCTTCATCCTGTTCCTGCTGGATGTG-3′), SAP505 (5′-phosphate-ATCCCGTATTGATGCCGGGCAAGAGC-3′), and BsaHI, respectively. The mutagenic and selection primers and restriction enzyme used to generate the $S1P_3$ mutation were SAP486 (5′-phosphate-CTCTTCATCCTGTTCCTGCTGGATGTG-3′), SAP506 (5′-phosphate-GACTGGTGAGTATTCAACCAAGTCATT-3′), and ScaI, respectively. The coding sequences of the $S1P_1$ Leu276Phe and $S1P_3$ Phe263Leu mutants were confirmed by DNA sequence analysis. For expression studies, the $S1P_1$ Leu276Phe mutant was cloned into pCDEF3neo as a BamHI-NotI fragment. The $S1P_3$ Phe263Leu mutant was subcloned into the EcoRI-NotI restriction sites of vector pCDEF3neo.

Transient Expression of the $S1P_1$ and $S1P_3$ Receptors. For expression studies with the $S1P_3$ receptor, CHO cells were plated at a density of 1.6×10^6 cells per 100-mm culture dish. After 24 h of incubation at 37°C, cells were transfected with 2 μg of $S1P_3$ plasmid DNA and 100 μg of Lipofectamine transfection reagent (Invitrogen) in serum-free Iscove's modified Dulbecco's medium (Invitrogen) supplemented with 1 mM sodium pyruvate and HT (0.1 mM sodium hypoxanthine and 16 μM thymidine) (Invitrogen) for 5 h at 37°C, per

the manufacturer's protocol. The transfection reaction was removed from the cell monolayer and replaced with Iscove's modified Dulbecco's medium containing sodium pyruvate, HT, and 10% charcoal/dextran-treated fetal bovine serum (Hyclone, Logan, UH). Transfected cells were allowed to recover for approximately 18 h at 37°C. Transient transfection experiments with the $S1P_1$ receptor were carried out in a similar manner with 8 μg of plasmid DNA.

Production of Stable Cell Lines Expressing S1P Receptors. CHO cells were transfected with plasmids encoding the $S1P_1$ and $S1P_3$ wild-type or mutant receptors, and clonal cell lines stably expressing the receptors were isolated in Iscove's modified Dulbecco's medium supplemented with sodium pyruvate, HT, 10% charcoal/dextran-treated fetal bovine serum after selection with G418. Stable CHO cell lines expressing the $S1P_1$ and $S1P_3$ receptors were identified in [^{33}P]S1P binding assays using whole cells and assay conditions described below.

Preparation of Membranes from Whole Cells. Cell membranes were prepared from whole cells, as described previously (Mandala et al., 2002). Protein concentrations were determined using the Bradford protein assay kit II (Bio-Rad Laboratories, Hercules, CA).

Competitive Ligand Binding Assays. Transiently transfected CHO cells expressing the S1P receptors were assayed for binding of [^{33}P]S1P (3000 Ci/mmol) using published procedures (Mandala et al., 2002), modified as follows. Transfected cells were dissociated from monolayer cultures in enzyme-free cell dissociation buffer (Specialty Media, Phillipsburg, NJ), collected by centrifugation at 400*g*, washed once with PBS, and resuspended in binding buffer (50 mM HEPES, 5 mM $MgCl_2$, 1 mM $CaCl_2$, 0.5% bovine serum albumin, and 1 mM sodium vanadate) at a concentration of 2.5×10^5 cells/ml. The binding reactions with whole cells were initiated by the addition of 100 μl of transfected cells (2.5×10^4) to 100 μl of 0.1 nM [^{33}P]S1P/unlabeled S1P ligand in 96-well multiscreen filtration plates (Millipore, Bedford, MA). The reactions were incubated at 22°C for 1 h. After ligand binding, the reactions were washed twice with 150 μl of unlabeled binding buffer, the assay plate was dried, and 100 μl of Microscint 20 (PerkinElmer Life and Analytical Sciences, Boston, MA) was added to each well. Plates were counted in a PerkinElmer Life and Analytical Sciences Microplate scintillation and luminescence counter or the Wallac Trilux 1450 Microbeta liquid scintillation and luminescence counter (PerkinElmer Life and Analytical Sciences). Competitive ligand binding assays with membranes prepared from stably transfected CHO cells and 0.1 nM [^{33}P]S1P/unlabeled S1P ligand were performed as described previously (Mandala et al., 2002). Assays of the $S1P_3$ receptors were performed with 0.25 μg of membrane protein. Western hybridization (see Fig. 6 under *Results*) and radioligand binding experiments titrating membrane protein concentration (data not shown) indicated that the $S1P_1$ Leu276Phe receptor was expressed at a higher density than the wild-type receptor in the stable CHO cell lines. Competition binding assays of the $S1P_1$ wild-type and $S1P_1$ Leu276Phe receptors were performed with 0.57 and 0.285 μg, respectively. Binding experiments were performed in triplicate in three separate experiments. Data were analyzed by nonlinear regression using a one-site competition model in the program Prism (GraphPad Software, San Diego, CA) to determine Log IC_{50}. The Log IC_{50} values from each experiment were analyzed in an unpaired Student's *t* test.

S1P Saturation Binding Assays. The K_d and B_{max} values of mutant and wild-type receptors in membrane fractions from the stable CHO cell lines expressing the $S1P_1$ or $S1P_3$ receptors were determined in saturation binding assays with [^{33}P]S1P (3000 Ci/mmol) in two experiments performed in triplicate. A cocktail of unlabeled S1P and [^{33}P]S1P ligand was titrated in triplicate in a six-point titration, ranging from 3 nM S1P to 0.025 nM in binding buffer. In prewetted 96-well multiscreen filtration plates (Millipore, Medford, MA), 100 μl of each ligand dilution was added to each reaction well. Two microliters of 50 μM unlabeled S1P was added to a parallel set of reactions to determine nonspecific binding. Reactions were initiated by the addition of membrane fractions, incubated at 22°C for 1 h, and washed twice with 150 μl of chilled binding buffer. After drying assay plates at 40°C for 1 h, 100 μl of Microscint 20 (PerkinElmer Life and Analytical Sciences) was added to each well and the plates were counted in a Wallac Trilux 1450 Microbeta liquid scintillation and luminescence counter (PerkinElmer Life and Analytical Sciences). Data were analyzed by nonlinear regression and fit to a one-site binding model using the program Prism to determine the K_d and B_{max} values (GraphPad Software).

Measurements of [^{35}S]GTPγS Binding. [^{35}S]GTPγS (1250 Ci/mmol) binding was assayed in membranes (3 μg) prepared from CHO cell lines as described previously (Mandala et al., 2002). The reactions were incubated at 22°C for 1 h and washed six times with distilled water using a Filtermate Harvester (PerkinElmer Life and Analytical Sciences). After drying the reaction plates at 50°C, 50 μl of ScintiSafe Plus 50% (Fisher Scientific Co., Pittsburgh, PA) was added to each well, and the plates were counted in a Microplate scintillation and luminescence counter or a Wallac Trilux 1450 Microbeta liquid scintillation and luminescence counter. [^{35}S]GTPγS binding assays were performed in triplicate in three separate experiments. Data were analyzed by nonlinear regression and fit to a sigmoidal dose-response curve using the program Prism (GraphPad Software) to determine the Log EC_{50} values. The Log EC_{50} values of individual compounds for the wild-type and mutant receptors were analyzed in an unpaired Student's *t* test. The efficacies (E_{max}) of the agonists tested to stimulate [^{35}S]GTPγS binding were calculated as the percentage of the maximal increase obtained using 5 μM S1P on the wild-type $S1P_1$ or $S1P_3$ receptors.

$S1P_1$ and $S1P_3$ Antisera. The C-terminal $S1P_1$ rabbit antiserum MS1766 has been described previously (Forrest et al., 2004). A peptide in the N terminus of human $S1P_3$ (REHYQYVGKLAGRLKEASE) was synthesized (SynPep Corp, Dublin, CA), conjugated to keyhole limpet hemocyanin, and used to immunize rabbits (Covance Research Products, Denver, PA). Specific IgG fractions were affinity purified using the immunizing peptide and tested by Western hybridization against a panel of human, mouse, and rat S1P receptors. The $S1P_3$ antiserum MS2284 was specific for the human $S1P_3$ receptor.

Confocal Microscopy Studies of $S1P_1$ and $S1P_3$ Receptor Expression. Stable CHO clones expressing the receptors were plated in four chambers of the Lab-Tek II Chamber 1.5 German Coverglass System at a density of 40,000 cells per chamber, in Iscove's modified Dulbecco's medium with sodium pyruvate, HT, 10% charcoal/dextran-treated fetal bovine serum, and 25 mM HEPES buffer, pH 7.5. Cells were allowed to adhere for 24 h at 37°C. Growth medium was removed and cells were washed/equilibrated with FACS buffer (1× PBS containing 2.5% charcoal/dextran-treated fetal bovine serum, 25 mM HEPES, and 0.05% NaN_3). To detect $S1P_3$, adherent cells were blocked with goat IgG blocking antibody (MP Biomedicals, Irvine, CA) at 100 μg/ml in FACS buffer. After 10 min of incubation at 22°C, cells were incubated with receptor-specific antisera, including a rabbit $S1P_1$ antiserum (MS1766) or a rabbit $S1P_3$ antiserum (MS2284) at 100 μg/ml in a 200-μl reaction volume. A normal rabbit anti-IgG antibody (Santa Cruz Biotechnology, Santa Cruz, CA) served as the isotype control. In addition, the fourth chamber of cells did not receive antibody and served as the nonspecific fluorescence control. Cells were incubated for 30 min at 22°C, followed by 2 washes with FACS buffer. Cells were then incubated with a secondary goat anti-rabbit IgG fluorescein isothiocyanate-labeled antibody (Santa Cruz Biotechnology) at 25 μg/ml for 30 min at 22°C. Cells were washed two times with FACS buffer, fixed with BD Cytofix/Cytoperm solution (BD Biosciences Pharmingen, San Diego, CA), and washed with BD Perm/Wash solution (BD Biosciences Pharmingen) that was diluted in FACS buffer according to the manufacturer's protocol. The stained cells were then washed with FACS buffer, washed twice with PBS, overlaid with PBS containing 5 nM DRAQ5 (Biostatus Limited, Leicestershire, UK) and viewed by confocal microscopy.

To detect $S1P_1$, adherent cells were washed with FACS buffer and fixed/permeablized in BD Cytofix/Cytoperm solution according to the manufacturer's protocol. Cells were washed and maintained in BD Perm/Wash buffer. Cells were then hybridized with MS1766 or MS2284 and viewed by confocal microscopy according to the same procedure described for detection of $S1P_3$.

Western Hybridization Analysis of $S1P_1$ and $S1P_3$ Receptor Expression. Membrane fractions from stable CHO cells expressing the S1P receptors were separated on 12% Precise Protein Gels (Pierce, Rockford, IL). Precision Plus Protein Standards (Bio-Rad Laboratories) were electrophoresed in adjacent wells for size determinations. Proteins were transferred to a 0.45-μm Immobilon-P PVDF membrane (Millipore, Billerica, MA) for 2 h at 75 V. The membranes were washed with 1× Tris-buffered saline + 0.05% Tween 20 (which was also included in all subsequent wash steps) and blocked with starting block (Tris-buffered saline) blocking buffer (Pierce) containing 0.05% Tween 20. Hybridization of rabbit $S1P_1$ antiserum (MS1766; 1:1000 dilution) or rabbit $S1P_3$ antiserum (MS2844; 1:3000) was performed in Starting Block buffer at 4°C for 16 h. After three 5-min washes, the membranes were incubated with a stabilized goat anti-rabbit IgG-HRP conjugated antibody (Pierce) at a 1:3000 dilution ($S1P_1$) or 1:20,000 dilution ($S1P_3$) for 1 h at 22°C. Hybridization was detected with the Pierce ECL-femto kit following the manufacturer's protocol, using CL-X Posure film (Pierce).

Results

Homology Modeling of the $S1P_1$ and $S1P_3$ Receptors. To model the structures of the S1P receptors, we aligned their primary amino acid sequences with other members of the GPCR A subfamily to optimize the sequence alignment. Bovine rhodopsin was used as the structural template for the homology model. The alignment of TMs 3 to 7 of S1P receptors with bovine rhodopsin is illustrated in Fig. 2. The most conserved residues in the family A GPCRs are conserved in six of the seven TM domains in S1P receptors, except TM5. The most highly conserved Pro (5.50) in TM5 of the family A GPCRs is replaced by hydrophobic residues in the S1P receptors (i.e., Leu in $S1P_1$, Ile in $S1P_2$, $S1P_3$ and $S1P_5$, and Val in $S1P_4$) (Fig. 2). However, another highly conserved residue, Tyr (5.58) (Bosch et al., 2005), is present in all five S1P receptors. In many of the family A GPCRs, a disulfide bond exists between TM3 and the second extracellular loop between TM4 and TM5 (Bosch et al., 2005). For example, in bovine rhodopsin, the disulfide bond is formed between residue Cys110(3.25) and Cys187 (Palczewski et al., 2000). This disulfide bond does not exist in the S1P receptors, which contain a Trp in TM3 in place of Cys at position 3.25.

The $S1P_1$ and $S1P_3$ receptors share the highest degree of amino acid sequence relatedness in the S1P receptor family, with approximately 50% of the residues identical, another 20% of the residues strongly similar, and more than 10% of the residues weakly similar. Because the $S1P_1$ and $S1P_3$ receptors are highly conserved, the $S1P_1$ homology model was used for docking of agonists. The $S1P_1$ homology model displays a three-dimensional structure similar to that of bovine rhodopsin, with a 7TM helical bundle and a short cytoplasmic helix (Fig. 3). The $S1P_3$ receptor was modeled based on the $S1P_1$ homology model, focusing on the nonconserved residues.

Structure of the Agonist Binding Pocket of the $S1P_1$ and $S1P_3$ Receptors. The compounds used in this study included the natural ligand S1P, FTY720-P (a phosphate ester of FTY720), and compounds A and B, which are $S1P_1$-selective agonists (Fig. 1). These compounds share common structural characteristics including charged head groups and long lipophilic side chains. The *S*-enantiomeric phosphate ester of FTY720-P was used to generate models of agonist-bound $S1P_1$ receptor complexes for several reasons. It is a more potent agonist of the human $S1P_1$ receptor than the *R*-enantiomer (Hale et al., 2004b) and is an agonist of $S1P_3$, $S1P_4$, and $S1P_5$. The *R*-enantiomer is a full agonist of $S1P_1$ and $S1P_4$ but its potency at these receptors is lower and it is

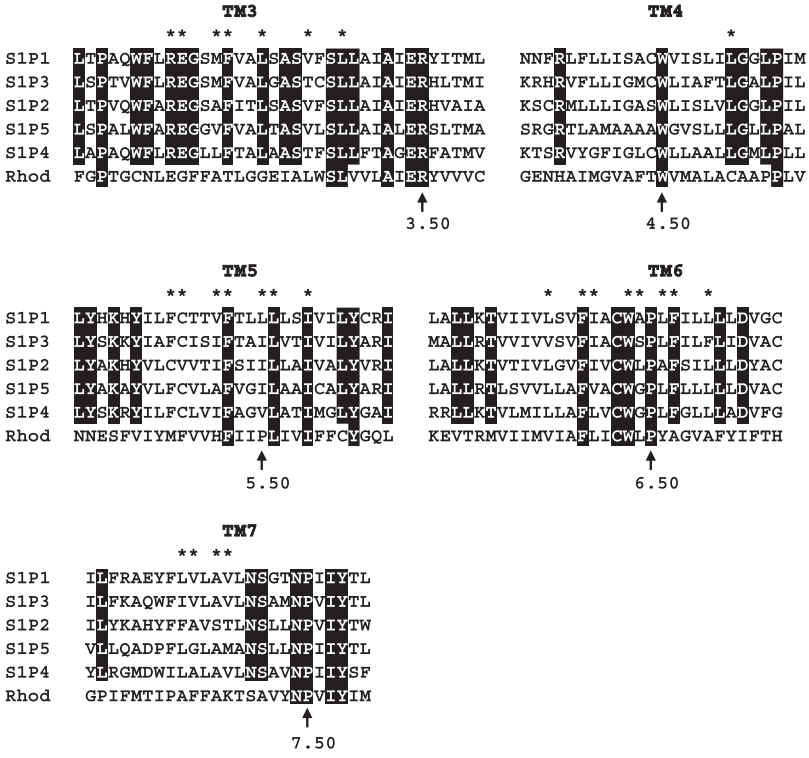

Fig. 2. Alignment of amino acid sequences of TM3, TM4, TM5, TM6, and TM7 in the S1P receptors with bovine rhodopsin. Conserved residues are shown in black boxes. The most conserved residues in each helix are marked by an arrow and labeled with the Ballesteros-Weinstein index. Residues that are also conserved in the TM helices of rhodopsin are also shaded in black. Asterisks above the alignments denote residues predicted to be located within 4 Å of ligand in the docking models of $S1P_1$ with S1P, FTY720-P, compound A, or compound B.

an antagonist of $S1P_3$ and $S1P_5$. At the time these experiments were initiated, the agonist/antagonist activities and affinities of the enantiomeric phosphate esters of S1P against the S1P receptor family were also unknown.

In the agonist docking models, S1P, FTY720-P, and the $S1P_1$-selective compounds A and B bind to a common pocket that contains conserved receptor-agonist interactions. The preferred docking mode for agonists in these models is depicted in Fig. 3, in which FTY720-P is illustrated. The agonists are bound in the upper half of the TM helical bundle, toward the extracellular surface. The agonists have an extended conformation in a narrow binding pocket and are surrounded by residues mainly from TMs 3, 5, and 6, and a few residues from TMs 4 and 7. Amino acid residues with any atom located within 4 Å of ligands in the docking models are indicated with asterisks in Fig. 2 and are highlighted in green or yellow [Leu276(6.55)] in Fig. 3.

Further examination of receptor residues within 4 Å of the agonists in the binding pocket identified two groups of interactions (Fig. 4). The first group consists of the charged residues on TM3, Arg120(3.28) and Glu121(3.29), identified by Parrill and colleagues (Parrill et al., 2000; Inagaki et al., 2005; Jo et al., 2005). These receptor residues interact with the charged head groups of agonists in our models. For example, the distance between the anionic phosphate group of FTY720-P and the positively charged side chain of Arg120(3.28) of $S1P_1$ is approximately 2.5 Å; likewise, the ammonium of FTY720-P is within 2.6 Å of the negatively charged side chain of Glu121(3.29) (Fig. 4B). The second group of interactions consists of nine aromatic and hydrophobic amino acids, adjacent to the lipophilic side chains of the agonists. These residues include Phe125(3.33), Leu128(3.36), Phe205(5.42), Phe210(5.47), Phe265(6.44), Trp269(6.48), Leu272(6.51), Phe273(6.52), and Leu276(6.55). Eight of these residues are conserved between $S1P_1$ and $S1P_3$ receptors. The ninth residue, Leu276(6.55) in $S1P_1$, is replaced by Phe263(6.55) in $S1P_3$ (Fig. 2). In the $S1P_1$-agonist docking models, Leu276(6.55) forms van der Waals interactions with the phenyl ring and azetidine of compounds A and B (Fig. 4, C and D). In the $S1P_3$ model, the bulkier Phe263 residue reduces the size of the binding pocket and sterically hinders binding of compounds A and B to the receptor. These results suggested that the Leu276/Phe263 residues contribute to the $S1P_1$/$S1P_3$ selectivity of compounds A and B.

$S1P_1$ and $S1P_3$ Receptor Binding Assays. We developed a competitive receptor binding assay using CHO cells transiently transfected with the $S1P_1$ and $S1P_3$ receptors to rapidly assay agonist binding to the receptor mutants. In this assay, S1P inhibited the binding of [^{33}P]S1P to the $S1P_1$ and $S1P_3$ receptors with high affinity (Fig. 5, A and B). When assayed in binding assays using transiently transfected receptors, compound A bound $S1P_1$ with high affinity and exhibited selectivity for $S1P_1$ over $S1P_3$ (Fig. 5).

To investigate the role of the $S1P_1$ Leu276 and $S1P_3$ Phe263 residues in the selectivity of compound A, we constructed $S1P_1$ Leu276Phe and $S1P_3$ Phe263Leu mutant receptors by site-directed mutagenesis and assayed the abilities of the receptors to bind S1P and compound A in transiently transfected cells. The $S1P_1$ Leu276Phe and $S1P_3$ Phe263Leu mutants bound S1P with high affinities similar to those of the wild-type receptors (Fig. 5). The $S1P_1$-selective compound A bound to the $S1P_1$ Leu276Phe mutant receptor with lower affinity compared with the wild-type $S1P_1$ receptor. Conversely, the $S1P_3$ Phe263Leu mutant receptor bound to compound A with higher affinity compared with the wild-type $S1P_3$ receptor.

Wild-Type and Mutant S1P Receptors Are Expressed on the Cell Surface of Stable Cell Lines. Stable CHO cell lines expressing the wild-type and mutant $S1P_1$ and $S1P_3$ receptors were generated to expand the characterization of the mutant $S1P_1$ Leu276Phe and $S1P_3$ Phe263Leu receptors. Expression patterns of the wild-type and mutant receptors in the stable cell lines were characterized by Western hybridization and confocal microscopy. Murine $S1P_1$ is *N*-glycosylated in the ectodomain on an asparagine residue in CHO cell lines overexpressing the receptor, and this residue is conserved in $S1P_2$, $S1P_4$, and $S1P_5$ (Kohno et al., 2002). The amino-terminal ectodomains of murine $S1P_1$ and $S1P_3$ are also truncated in overexpressing CHO cells (Kohno and Igarashi, 2003). We have observed similar findings with the

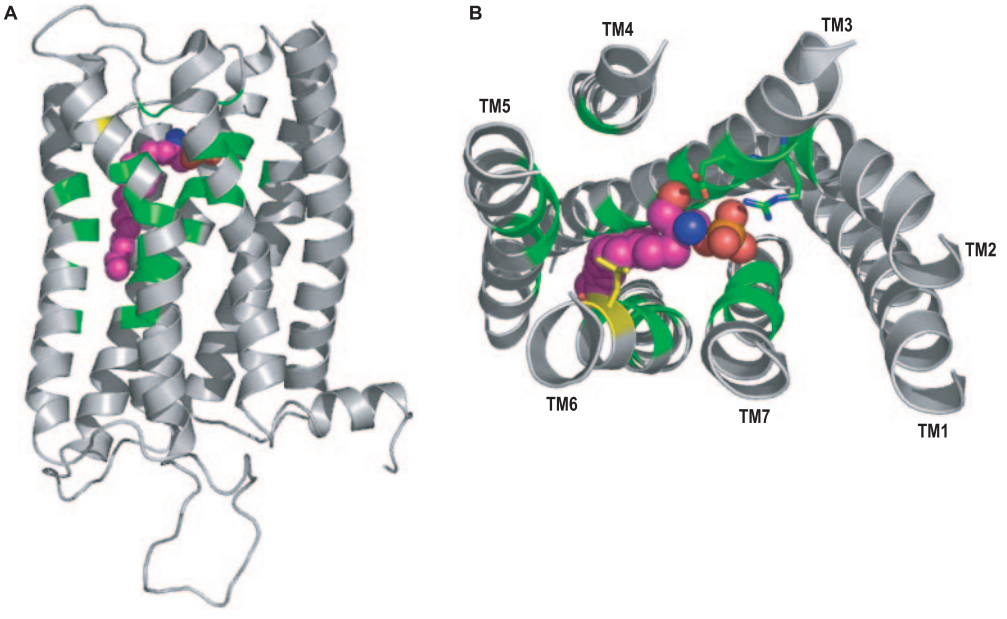

Fig. 3. Docking model of $S1P_1$ in complex with FTY720-P. A, the TM structures of $S1P_1$ are shown as gray ribbons with residues located within 4 Å of the agonist highlighted in green and Leu276(6.55) highlighted in yellow. FTY720-P is shown in a spheres model, with carbon in purple, oxygen in red, nitrogen in blue, and phosphorus in orange. The hydrogen atoms are omitted for clarity. B, a perpendicular view of the TM helices of $S1P_1$ in complex with FTY720-P. The loop regions and the cytoplasmic helix were removed for clarity. The TM helices are shown as gray ribbons with residues located within 4 Å of ligand highlighted in green and Leu276(6.55) highlighted in yellow. The side chains of Arg120 (3.28) and Glu121(3.29) are shown in stick form with carbon atoms in green, oxygen atoms in red, and nitrogen atoms in blue. Leu276(6.55) is shown in stick form in yellow. The pictures were prepared by PyMOL (DeLano Scientific LLC, South San Francisco, CA).

stable cell lines expressing the human wild-type and mutant $S1P_1$ and $S1P_3$ receptors. The predicted size of the flag-tagged human $S1P_1$ receptors in these experiments is 44.3 kDa. The $S1P_1$-specific antiserum recognizes proteins of approximately 54.3, 49.2, and 44.5 kDa in membranes prepared from the cell lines expressing the wild-type receptor and proteins of approximately 54.3 and 49.2 kDa in membranes prepared from the cell line expressing the Leu276Phe $S1P_1$ receptor (Fig. 6A). Results from these experiments indicate that the stable cell line expressing the $S1P_1$ Leu276Phe receptor expressed approximately 5-fold more receptor than the cell line expressing the wild-type receptor. The sizes of the human $S1P_1$ wild-type and Leu276Phe receptors expressed in CHO cells indicate that these receptors are glycosylated. We have also observed that the wild-type and mutant $S1P_1$ receptors do not cross-react with an antibody that recognizes the Flag tag (data not shown), indicating that human $S1P_1$ receptors are also truncated at the N terminus. Proteins of approximately 47.7 kDa were detected in membranes from the cell lines expressing the $S1P_3$ wild-type and Phe263Leu receptors (Fig. 6B). The predicted sizes of the flag-tagged $S1P_3$ receptors are 43.8 kDa, suggesting that the receptors are migrating anomalously or are post-translationally modified. The wild-type and mutant $S1P_3$ receptors were also not recognized by the Flag antibody (data not shown), indicating that the human $S1P_3$ receptors are also truncated at the N terminus.

We also examined localization of the wild-type and mutant receptors by confocal microscopy (Fig. 7). The $S1P_1$ antiserum recognized $S1P_1$ wild-type or Leu276Phe mutant receptors at the cell surface, indicating that the Leu276Phe mutation did not alter trafficking of the receptor in cells. Similar results were obtained when localization of the $S1P_3$ wild-type and Phe263Leu mutant receptors were examined with the $S1P_3$ antiserum.

The $S1P_1$ Leu276Phe and $S1P_3$ Phe263Leu Mutations Alter the Binding Affinities and Agonist Activities of Compounds A and B. The K_d and B_{max} of the wild-type and mutant receptors in membranes prepared from the stable cell lines were also determined in saturation binding assays with [^{33}P]S1P (Table 1). The K_d values for the $S1P_1$ wild-type and Leu276Phe receptors were 0.39 and 0.29 nM, respectively. In these experiments, the B_{max} values of the wild-type and mutant receptors were 9.26 and 13.89 fmoles/μg, respec-

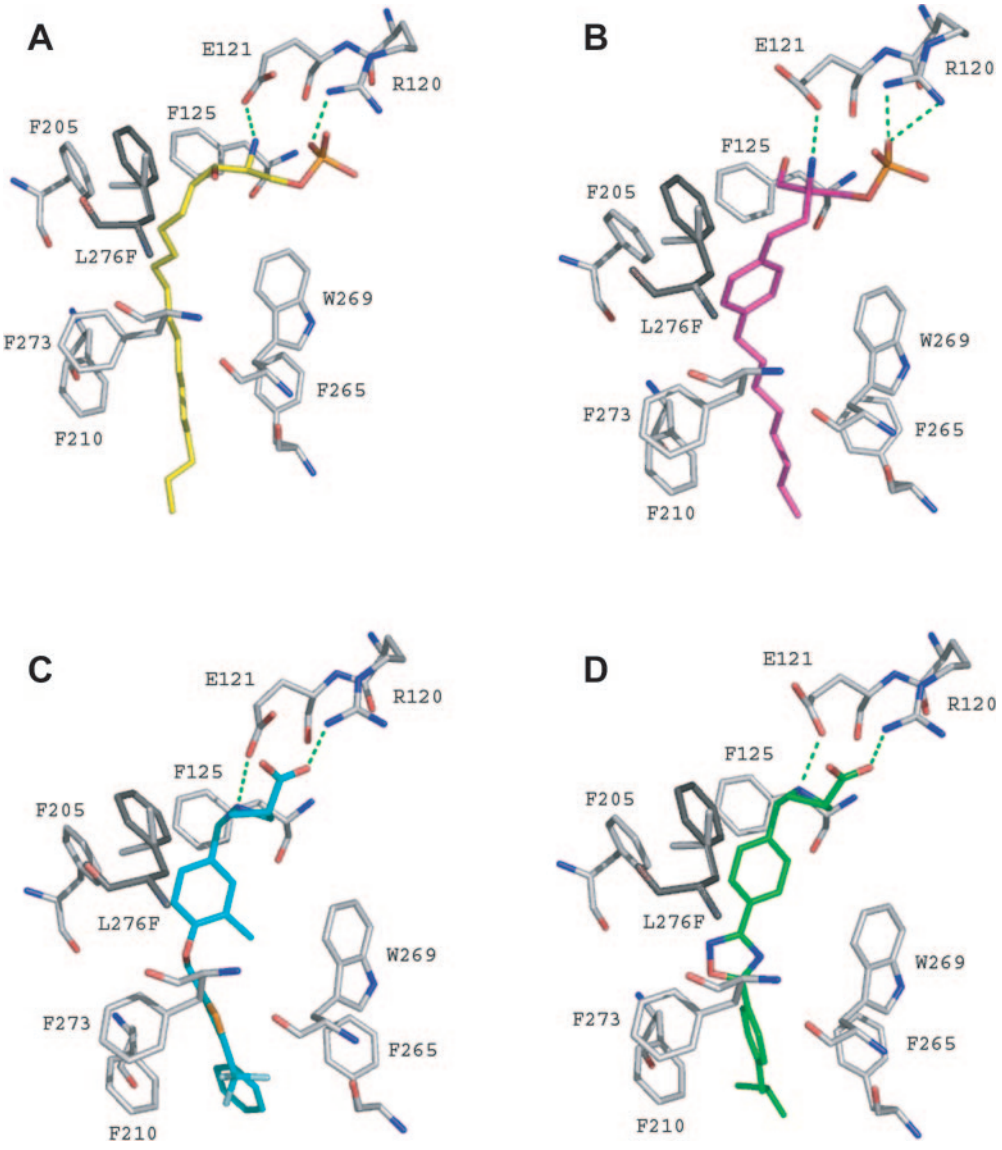

Fig. 4. A closer look at agonists in the $S1P_1$ binding site. Agonists are shown in stick form with carbons in S1P in yellow (A), FTY720-P in purple (B), compound A in cyan (C), and compound B in green (D). Hydrogen atoms are omitted for clarity. Six aromatic residues and Leu276(6.55) in the binding pocket of $S1P_1$ receptor are shown as gray sticks. For comparison, a Phe residue is depicted in black and overlaid onto the Leu276(6.55) of $S1P_1$ to model Phe263(6.55) in $S1P_3$. Oxygen atoms are depicted in red, nitrogen atoms in blue, and phosphorus atoms in orange. The dashed lines illustrate atom pairs within hydrogen bond distance, indicating favorable interactions between the head group of the agonists and the charged residues Arg120(3.28) and Glu121(3.29) on TM3. The pictures were prepared by PyMOL (DeLano Scientific LLC).

tively, indicating that the receptor density of the mutant receptor is higher than that of wild-type $S1P_1$. These results indicate that the Leu276Phe mutation in $S1P_1$ does not alter the conformation of the receptor dramatically resulting in a large change in affinity for the ligand. Similar results were observed in saturation binding assays with the $S1P_3$ wild-type and Phe263Leu mutant receptors. The K_d values for the $S1P_3$ wild-type and Phe263Leu receptors were 0.23 and 0.22 nM, respectively. The B_{max} values of the stable cell line expressing the wild-type and mutant $S1P_3$ receptors were 14.24 and 15.98 fmol/μg, respectively.

The affinities of S1P, FTY720-P, compound A, and compound B for the wild-type and mutant receptors were assayed in competitive binding assays with membrane fractions prepared from stable clones expressing the wild-type and mutant receptors. Log IC_{50} values are indicated in Table 2. Unlabeled S1P competed [^{33}P]S1P from the wild-type and mutant $S1P_1$ receptors with similar high affinities (Log IC_{50} values of -9.20 and -9.29 M, respectively). FTY720-P also competed [^{33}P]S1P from the wild-type and mutant $S1P_1$ receptors with Log IC_{50} values of -8.96 and -8.88 M, respectively. The affinities of S1P and FTY720-P for the wild-type and mutant $S1P_3$ receptors were also comparable. S1P competed [^{33}P]S1P from the wild-type and mutant $S1P_3$ receptors with Log IC_{50} values of -9.35 and -9.29 M, respectively, whereas FTY720-P competed [^{33}P]S1P from these receptors with Log IC_{50} values of -8.57 and -8.41 M, respectively.

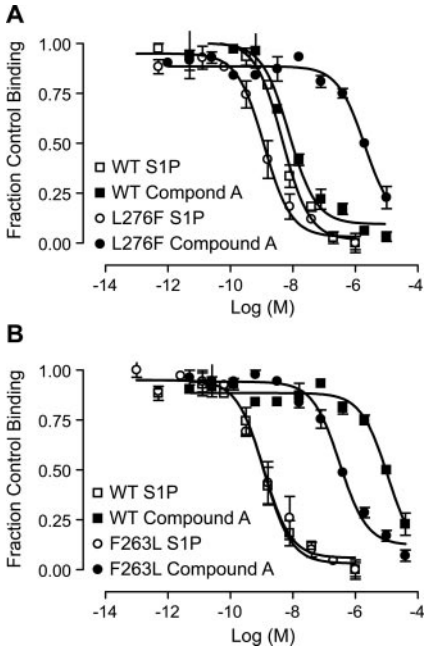

Fig. 5. The $S1P_1$Leu276Phe and $S1P_3$ Phe263Leu mutations specifically alter the affinity of the $S1P_1$ and $S1P_3$ receptors for compound A. A, data are from a representative competitive binding experiment with CHO cells transiently transfected with the wild-type or mutant $S1P_1$ receptors. Results (mean ± range, $n = 2$) are from duplicate determinations in a single experiment and are plotted as the fraction of control binding versus the logarithm of the concentration of the competitor. Similar agonist affinities were seen in several experiments. B, data are from a representative competitive binding experiment with CHO cells transiently transfected with the wild-type or mutant $S1P_3$ receptors. Results (mean ± range, $n = 2$) are from duplicate determinations in a single experiment and are plotted as the fraction of control binding versus the logarithm of the concentration of the competitor. Similar agonist affinities were seen in several experiments.

To examine the contribution of $S1P_1$ Leu276 and $S1P_3$ Phe263 residues to $S1P_1$-selective compounds A and B, we determined the Log IC_{50} values of these compounds for the wild-type and mutant $S1P_1$ and $S1P_3$ receptors (Table 2). Compound A bound to the wild-type $S1P_1$ receptor with approximately 13-fold higher affinity than to the $S1P_1$ Leu276Phe receptor. The Log IC_{50} of compound A on the mutant receptor was -7.37 M. The $S1P_1$-selective agonist compound B bound to wild-type $S1P_1$ receptor with approximately 40-fold higher affinity than to the Leu276Phe mutant with a Log IC_{50} of -7.33 M. In contrast, the $S1P_1$-selective compounds bound with approximately 10- and 151-fold higher affinities to the mutant $S1P_3$ Phe263Leu receptor compared with the wild-type receptor. The Log IC_{50} values of compounds A and B for the $S1P_3$ Phe263Leu mutant were -6.71 and -7.56 M, respectively.

The potencies and efficacies of S1P, FTY720-P, and compounds A and B for the wild-type and mutant receptors were also evaluated in [^{35}S]GTPγS binding assays (Fig. 8 and Table 3). The basal activities (mean ± S.E.) of the $S1P_1$ wild-type and mutant receptors were 1102 ± 137 and 862 ± 51 fmol/mg, respectively, and S1P activated the receptors with similar affinities (Log EC_{50} of -7.48 and -7.58 M, respectively). In our in vitro experiments measuring [^{35}S]GTPγS binding, the potency of S1P as an agonist of the S1P wild-type and mutant receptors is approximately 50-fold lower than the affinity of S1P for these receptors in competition binding assays. This decrease in potency is due to a phosphatase activity in CHO membrane preparations overexpressing the $S1P_1$ receptor (J. Milligan, G. J. Shei and S. Mandala, data not shown). This activity hydrolyzes S1P,

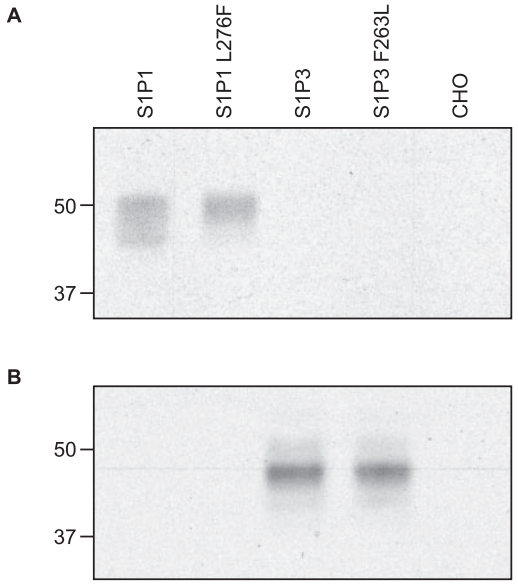

Fig. 6. Expression of the $S1P_1$ Leu276Phe and $S1P_3$ Phe263Leu receptors. A, Western hybridization analysis of wild-type and mutant $S1P_1$ and $S1P_3$ receptors expressed in stable CHO cell lines with $S1P_1$ antiserum. The following amounts of membrane protein were electrophoresed on the gel: 1 μg of $S1P_1$, 0.2 μg of $S1P_1$ Leu276Phe, 1 μg of $S1P_3$, 1 μg of $S1P_3$ Phe263Leu, and 1 μg of CHO control membrane protein. B, Western hybridization analysis of wild-type and mutant $S1P_1$ and $S1P_3$ receptors expressed in stable CHO cell lines with $S1P_3$ antiserum. The following amounts of membrane protein were electrophoresed: 4 μg of $S1P_1$, 1 μg of $S1P_1$ Leu276Phe, 1 μg of $S1P_3$, 1 μg of $S1P_3$ Phe263Leu, and 1 μg of CHO control membrane protein.

resulting in a loss of potency of the natural agonist in the [^{35}S]GTPγS binding assay. S1P also induced a significant agonist response by the mutant receptor (E_{max}, 115%). The basal activities (mean ± S.E.) of the $S1P_3$ wild-type, and mutant receptors were 1555 ± 73 and 2065 ± 50 fmol/mg, respectively. The Log EC_{50} values of S1P for the wild-type and mutant $S1P_3$ receptors were −8.45 and −8.64 M, respectively, and S1P activated the $S1P_3$ mutant receptor efficiently (E_{max} 82%). The $S1P_3$ Phe263Leu mutation had minimal effects on the basal activity of the receptor (Fig. 8). Although FTY720-P was a potent and efficacious agonist of the mutant $S1P_1$ Leu276Phe receptor (Log EC_{50} = −8.76 M, E_{max} = 109%), the compound was a 6-fold more potent agonist of the wild-type receptor (Log EC_{50} = −9.54 M, E_{max} = 95%). FTY720-P was also a potent agonist of the wild-type and mutant $S1P_3$ receptors with Log EC_{50} values of −8.87 and −9.07 M, respectively. This synthetic agonist also activated the wild-type and mutant $S1P_3$ receptors effectively with E_{max} values of 106 and 93%, respectively.

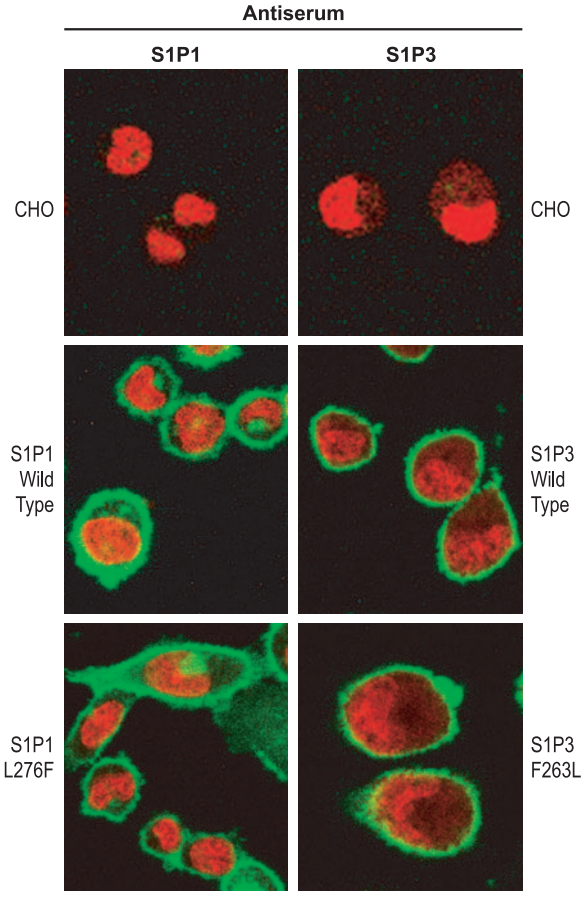

Fig. 7. Localization of the $S1P_1$ Leu276Phe and $S1P_3$ Phe263Leu receptors. Stable CHO cell lines expressing the wild-type or mutant $S1P_1$ and $S1P_3$ receptors were prepared for immunohistochemistry and confocal microscopy as described under *Materials and Methods*. Left, cells treated with the $S1P_1$ antiserum; right, cells treated with the $S1P_3$ antiserum. Top, control CHO cells transfected with a vector plasmid.

TABLE 1

Effects of Leu276Phe and Phe263Leu point mutations on the binding of S1P to the $S1P_1$ and $S1P_3$ receptors

K_d and B_{max} were determined in saturation binding assays with [^{33}P]S1P (3000 Ci/mmol) as described under *Materials and Methods*. Data were analyzed by nonlinear regression and fit to a one-site binding model using the program Prism (GraphPad Software). Results are expressed as the mean ± range of two experiments performed in triplicate.

Receptor	K_d	B_{max}
	nM	*fmol / μg*
$S1P_1$	0.39 ± 0.04	9.26 ± 0.08
$S1P_1$ Leu276Phe	0.29 ± 0.01	13.89 ± 0.33
$S1P_3$	0.23 ± 0.08	14.24 ± 1.78
$S1P_3$ Phe263Leu	0.22 ± 0.04	15.98 ± 1.40

The $S1P_1$ Leu276Phe and $S1P_3$ Phe263Leu mutations had significant affects on the agonist potencies of compounds A and B (Fig. 8 and Table 3). The $S1P_1$-selective compounds A and B were potent and efficacious agonists of the wild-type $S1P_1$ receptor. The Log EC_{50} values of the compounds were −8.81 and −9.61 M, respectively. The potencies of $S1P_1$-selective compounds A and B for the $S1P_1$ Leu276Phe mutant were lower compared with the wild-type receptor with Log EC_{50} values of −6.90 and −6.66 M, respectively. Despite a decrease in potency, compounds A and B activated the mutant $S1P_1$ receptor effectively with E_{max} values of 103 and 116%, respectively. In contrast, compounds A and B were more potent agonists of the $S1P_3$ Phe263Leu mutant compared with the wild-type $S1P_3$ receptor. The Log EC_{50} values of the compounds against the wild-type $S1P_3$ receptor were −6.34 and −5.85 M, respectively. Both $S1P_1$-selective agonists were more potent agonists of the $S1P_3$ Phe263Leu receptor, with Log EC_{50} values of −7.97 and −8.98 M, respectively. Both compounds A and B were also effective agonists of the wild-type and mutant $S1P_3$ receptors with E_{max} values ranging from 80 to 128%.

Discussion

The S1P receptors share high homology in their primary sequences and, as expected, the agonist binding pockets of the $S1P_1$ and $S1P_3$ receptors predicted by our modeling studies overlap and share conserved residues that interact with agonists. This is consistent with findings that many S1P receptor agonists do not exhibit significant receptor subtype selectivity. The potential clinical advantage of S1P receptor agonists lacking $S1P_3$ activity has prompted development of $S1P_1$/$S1P_3$ selective agonists and led us to study receptor-agonist interactions and receptor structural features that contribute to $S1P_1$/$S1P_3$ selectivity. Our modeling studies and mutagenesis experiments indicate that Leu276(6.55) in $S1P_1$ and Phe263(6.55) in $S1P_3$ are critical residues that contribute to the $S1P_1$-selectivity of compounds A and B.

In our docking models, the agonists bind $S1P_1$ in a narrow cavity located in the upper half of the 7TM helical bundle. The binding pocket consists of residues located on TMs 3, 5, 6, and 7. Similar pockets have been identified in many GPCRs by mutagenesis studies and are regarded as a common feature for family A GPCRs (Bondensgaard et al., 2004). Interactions between charged residues on TM3 and charged agonists or antagonists are found in many GPCRs (Feighner et al., 1998; Shin et al., 2002). The importance of S1P interactions with Arg120(3.28) and Glu121(3.29) in the $S1P_1$ receptor were revealed by mutagenesis studies directed by a model generated from a theoretically calculated structure of bovine rhodopsin (Parrill et al., 2000). Our model, which is based on the X-ray structure of bovine rhodopsin in the dark state, and mutagenesis studies on the human $S1P_1$ and $S1P_3$ receptors confirm these findings (data not shown). The

charged residues at the top of the binding pocket interact with the counter-ions in the charged head groups of the agonists. These conserved residues (Fig. 2) play important roles in recognizing charged agonists in all S1P receptors. Arg120(3.28) is also conserved in LPA receptors, but Glu121(3.29) is substituted with a Gln in LPA receptors.

TABLE 2

The effects of the $S1P_1$ Leu276Phe, and $S1P_3$ Phe263Leu mutations on affinities of S1P, FTY720-P, compound A, and compound B

Compound affinities (Log IC_{50}) were calculated from [^{33}P]S1P binding dose response curves. Results are expressed as the mean ± S.E. of three experiments performed in triplicate.

Compound	Log IC_{50}			
	$S1P_1$	$S1P_1$ L276F	$S1P_3$	$S1P_3$ F263L
	M			
S1P	−9.20 ± 0.22	−9.29 ± 0.16	−9.35 ± 0.15	−9.29 ± 0.17
FTY720-P	−8.96 ± 0.08	−8.88 ± 0.04	−8.57 ± 0.19	−8.41 ± 0.13
Compound A	−8.49 ± 0.19	−7.37 ± 0.08*	−5.73 ± 0.15	−6.71 ± 0.03[§]
Compound B	−8.93 ± 0.04	−7.33 ± 0.05[¶]	−5.38 ± 0.15	−7.56 ± 0.05[†]

Significantly different from wild type:
* $P = 0.0055$.
[§] $P = 0.0028$.
[¶] $P = <0.0001$.
[†] $P = 0.0002$.

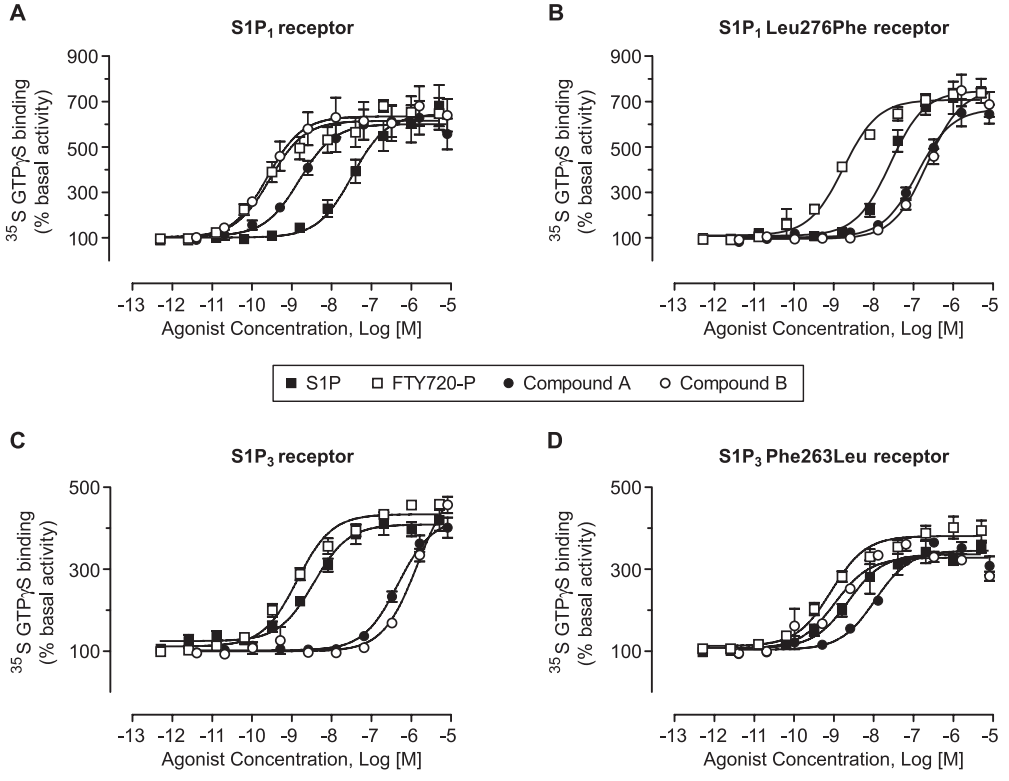

Fig. 8. The $S1P_1$ Leu276Phe and $S1P_3$ Phe263Leu mutations specifically alter the agonist potencies of compounds A and B. Data are from GTPγS binding experiments with membrane protein prepared from the stable cell lines expressing the wild-type or mutant S1P receptors. Results (mean ± S.E.) are from three experiments performed in triplicate and are plotted as the percentage basal activity versus the logarithm of the agonist concentration. A, $S1P_1$ receptor, basal activity = 1102 ± 137 fmol/mg. B, $S1P_1$ Leu276Phe mutant receptor, basal activity = 862 ± 51 fmol/mg. C, $S1P_3$ receptor, basal activity = 1555 ± 73 fmol/mg. D, $S1P_3$ Phe263Leu mutant receptor, basal activity = 2065 ± 50 fmol/mg.

TABLE 3

Effects of the $S1P_1$ Leu276Phe and $S1P_3$ Phe263Leu mutations on agonist activities of S1P, FTY720-P, compound A, and compound B

Agonist potencies (Log EC_{50}) were calculated from GTPγS binding dose response curves. Results are expressed as mean ± S.E. of three experiments performed in triplicate. The efficacies (E_{max}) of the agonists tested to stimulate GTPγS binding are expressed as the percentage of the maximal increase obtained with 5 μM S1P on the wild type $S1P_1$ or $S1P_3$ receptor.

	S1P		FTY720-P		Compound A		Compound B	
	Log EC_{50}	E_{max}	Log EC_{50}	E_{max}	Log EC_{50}	E_{max}	Log EC_{50}	E_{max}
	M	%	*M*	%	*M*	%	*M*	%
$S1P_1$	−7.48 ± 0.13	100	−9.54 ± 0.15	95	−8.81 ± 0.16	93	−9.61 ± 0.20	98
$S1P_1$ L276F	−7.58 ± 0.10	115	−8.76 ± 0.06[§]	109	−6.90 ± 0.08[¶]	103	−6.66 ± 0.09*	116
$S1P_3$	−8.45 ± 0.09	100	−8.87 ± 0.08	106	−6.34 ± 0.07	104	−5.85 ± 0.08	128
$S1P_3$ F263L	−8.64 ± 0.13	82	−9.07 ± 0.10	93	−7.97 ± 0.10*	85	−8.98 ± 0.16[†]	80

Significantly different from wild type:
[§] $P = 0.0083$.
[¶] $P = 0.0004$.
* $P = 0.0002$.
[†] $P < 0.0001$.

These LPA receptor residues are key determinants of their ligand specificity (Wang et al., 2001).

The hydrophobic domain of the proposed binding pocket of the $S1P_1$ receptor is adjacent to the lipophilic side chain of the agonists used in this study. Based on our docking models, a group of aromatic and hydrophobic residues lines the wall of the binding pocket. These residues are located deep in the pocket and provide important interactions with the lipophilic side chain of the agonists. Some of these residues, Phe125(3.33), Phe273(6.52), and Trp269(6.48), have also been proposed to interact with $S1P_1$ agonist SEW2871 (Jo et al., 2005). $S1P_1$ residues Phe210(5.47), Phe265(6.44), and Trp269(6.48) are among a group of highly conserved residues in many family A GPCRs (Bondensgaard et al., 2004). Previous mutagenesis studies illustrate the importance of aromatic residues in TM3 and -6 in the binding and activation of GPCRs by agonists (Spalding et al., 1998; Renzetti et al., 1999; Holst et al., 2004).

Our examination of the predicted agonist binding pockets of $S1P_1$ and $S1P_3$ identified a nonconserved Leu at position 6.55 in $S1P_1$. Four of five S1P receptors also contain a Leu at this position, whereas $S1P_3$ contains a Phe residue at the equivalent position. In our models, Leu276 in $S1P_1$ and Phe263 in $S1P_3$ affect the sizes of the binding pockets. The volume of the Phe aromatic side chain is approximately 25% larger than that of the aliphatic Leu side chain, making the $S1P_3$ binding pocket more crowded than the $S1P_1$ pocket. In the $S1P_1$ docking models, Leu276(6.55) is close to the phenyl ring and azetidine of $S1P_1$-selective compounds A and B (Fig. 4, C and D). The rigidity of these regions of compounds A and B makes it difficult for them to assume conformations that fit in the smaller binding pocket of the $S1P_3$ receptor, explaining their $S1P_1$ selectivity. When Leu276(6.55) is replaced with a Phe in the $S1P_1$ model, the binding pocket is smaller because of the bulkier size of the Phe side chain.

To test this model, we constructed $S1P_1$ and $S1P_3$ receptor mutants in which the Leu276 and Phe263 residues were exchanged and examined their expression and activity in Western hybridization, confocal microscopy, and radioligand binding experiments. These experiments indicate that the $S1P_3$ wild-type and mutant receptors are overexpressed on the surface of the stable CHO cell lines at similar densities and that both receptors bind S1P with high affinity. The K_d values of S1P for both receptors are approximately 0.2 nM. S1P binds the wild-type and mutant $S1P_1$ receptors with high affinity, with K_d values of 0.39 and 0.29 nM, respectively. The $S1P_1$ receptors are overexpressed on the surface of the stable CHO cells. Results from the Western hybridization experiments indicate that the mutant receptor is expressed at approximately 5-fold higher density than the wild-type receptor, whereas our ligand binding studies with [^{33}P]S1P indicate that the mutant receptor density is approximately 2-fold higher than the wild-type receptor. These results indicate that a fraction of the $S1P_1$ Leu276Phe receptors may be in a conformation that does not bind S1P with high affinity.

The competitive ligand binding and agonist functional studies comparing the $S1P_1$ and $S1P_3$ wild-type and mutant receptors confirm the predictions of the molecular models we developed for these receptors. The $S1P_1$ Leu276Phe mutant has a significantly reduced affinity for $S1P_1$-selective compounds A and B, and both of these agonists activate the $S1P_1$ mutant with much poorer potencies. On the other hand, substituting Phe263(6.55) of the $S1P_3$ receptor with Leu in the $S1P_3$ receptor enlarges the binding pocket of this mutant $S1P_3$ receptor, leading to an increase in the binding affinity and agonist potency of compounds A and B. This prediction was also verified experimentally with the $S1P_3$ Phe263Leu mutant. In addition, our conformational analyses of compounds A and B indicate that compound B is more rigid than compound A (data not shown), making it more difficult to assume a conformation that fits the binding pocket of the $S1P_3$ receptor and more susceptible to changes at Leu276 and Phe263 of the $S1P_1$ and $S1P_3$ receptors, respectively. Our in vitro analyses of the interactions of compounds A and B with the wild-type and mutant receptors demonstrate that the mutations have more dramatic effects on the binding affinity and agonist potency of compound B.

In contrast to $S1P_1$-selective compounds A and B, S1P contains a long, highly flexible alkyl side chain that easily adopts a conformation to bind to $S1P_1$ and $S1P_3$. It binds to both receptors with comparable affinities and is not sensitive to the Leu and Phe substitution mutations we constructed in $S1P_1$ and $S1P_3$. FTY720-P is also a high-affinity agonist of $S1P_1$ and $S1P_3$ with a slightly higher agonist potency against $S1P_1$. Our models predict that FTY720-P has a higher potency for $S1P_1$ because it contains a phenyl ring and prefers a larger binding pocket. The phenyl ring of FTY720-P is four bonds away from the positively charged ammonium group and seven bonds away from the negatively charged phosphate group. The longer linker between the charged head group and the phenyl ring of FTY720-P is more flexible than the azetidine moiety in $S1P_1$-selective compounds A and B. The models suggest that this flexibility is the reason FTY720-P is affected less by changes of the Leu276 and Phe263 residues in the binding pockets of $S1P_1$ and $S1P_3$. Although significant changes in FTY720-P binding affinity for the mutant or wild-type receptors were not observed in competition binding assays, the $S1P_1$ Leu276Phe mutation did confer a statistically significant change in agonist potency measured in vitro. FTY720-P activates the wild-type $S1P_1$ receptor 6-fold more potently than the $S1P_1$ Leu276Phe receptor, which contains a significantly smaller binding pocket.

These models predict that residues Leu276(6.55) and Phe263(6.55) are important contributors to $S1P_1$ and $S1P_3$ specificities of compounds A and B. However, the changes in agonist binding affinities and potencies observed with these mutations do not fully interconvert the pharmacological profiles of either agonist, indicating that other residues within the binding pocket also contribute to the specificities of these subtype-selective agonists. There are seven nonconserved residues in $S1P_1$ and $S1P_3$ within 4 Å of the predicted agonist binding pocket (Val3.40Thr, Val5.46Ile, Leu5.50Ile, Leu6.41Val, Ala6.49Ser, Leu6.55Phe, and Leu7.39Ile). Except for Leu276Phe, these residues are predicted to have smaller effects on the specificities of compounds A and B based on their positions and orientations. Combining the $S1P_1$ Leu276Phe or $S1P_3$ Phe263Leu mutations with amino acid substitutions in the other six nonconserved residues in $S1P_1$ and $S1P_3$ in the predicted agonist binding pocket may interconvert the pharmacological profiles of these agonists completely. Models of GPCR-agonist complexes based on X-ray crystal structures of rhodopsin in the unactivated "dark state" also have an inherent bias that might mask important receptor interactions with agonists.[2]

Our integrated molecular modeling and site-directed mutagenesis studies of the $S1P_1$ and $S1P_3$ receptors bound to

nonselective and $S1P_1$-selective agonists provide additional insights into the nature of different S1P receptor-agonist interactions and identify an important pair of residues in $S1P_1$ and $S1P_3$ that contribute significantly to receptor subtype selectivity of compounds A and B and FTY720-P. These findings provide a molecular basis for understanding $S1P_1/S1P_3$ subtype-selectivity of these S1P receptor agonists, which should aid development of more selective $S1P_1$ receptor agonists with immunosuppressive properties and improved safety profiles.

Acknowledgments

We are grateful to Hugh Rosen for encouragement and support in the early stages of this work. We thank James Milligan for synthesis of the radioligand used in the saturation binding assays, members of the Mandala laboratory for assay protocols and help in screening and characterizing antiserum MS2284, and Kevin Lynch for providing the expression plasmids encoding the human $S1P_1$ and $S1P_3$ receptors. We are also grateful to Michele McColgan and Sharon O'Brien for preparing the figures and Elizabeth Quackenbush for comments on the manuscript.

References

Archer E, Maigret B, Escrieut C, Pradayrol L, and Fourmy D (2003) Rhodopsin crystal: new template yielding realistic models of G-protein-coupled receptors. *Trends Pharmacol Sci* **24:**36–40.

Ballesteros JA and Weinstein H (1995) Integrated methods for the construction of three dimensional models and computational probing of structure-function relations in G-protein coupled receptors. *Methods Neurosci* **25:**366–428.

Bondensgaard K, Ankersen M, Thogersen H, Hansen BS, Wulff BS, and Bywater RP (2004) Recognition of privileged structures by G-protein coupled receptors. *J Med Chem* **47:**888–899.

Bosch L, Iarriccio L, and Garriga P (2005) New prospects for drug discovery from structural studies of rhodopsin. *Curr Pharm Des* **11:**2243–2256.

Budde K, Schmouder RL, Nashan B, Brunkhorst R, Lucker PW, Mayer T, Brookman L, Nedelman J, Skerjanec A, Bohler T, et al. (2003) Pharmacodynamics of single doses of the novel immunosuppressant FTY720 in stable renal transplant patients. *Am J Transplant* **3:**846–854.

Chiba K, Yanagawa Y, Masubuchi Y, Kataoka H, Kawaguchi T, Ohtsuki M, and Hoshino Y (1998) FTY720, a novel immunosuppressant, induces sequestration of circulating mature lymphocytes by acceleration of lymphocyte homing in rats. I. FTY720 selectively decreases the number of circulating mature lymphocytes by acceleration of lymphocyte homing. *J Immunol* **160:**5037–5044.

Chun J, Goetzl EJ, Hla T, Igarashi Y, Lynch KR, Moolenaar W, Pyne S, and Tigyi G (2002) International Union of Pharmacology. XXXIV. Lysophospholipid receptor nomenclature. *Pharmacol Rev* **54:**265–269.

Crippen GM and Havel TF (1988) *Distance Geometry and Molecular Conformation*, Wiley, New York.

Edwards PC, Li J, Burghammer M, McDowell JH, Villa C, Hargrave PA, and Schertler GF (2004) Crystals of native and modified bovine rhodopsins and their heavy atom derivatives. *J Mol Biol* **343:**1439–1450.

Fanelli F and De Benedetti PG (2005) Computational modeling approaches to structure-function analysis of G protein-coupled receptors. *Chem Rev* **105:**3297–3351.

Feighner SD, Howard AD, Prendergast K, Palyha OC, Hreniuk DL, Nargund R, Underwood D, Tata JR, Dean DC, Tan CP, et al. (1998) Structural requirements for the activation of the human growth hormone secretagogue receptor by peptide and nonpeptide secretagogues. *Mol Endocrinol* **12:**137–145.

Forrest M, Sun SY, Hajdu R, Bergstrom J, Card D, Doherty G, Hale J, Keohane C, Meyers C, Milligan J, et al. (2004) Immune cell regulation and cardiovascular effects of sphingosine 1-phosphate receptor agonists in rodents are mediated via distinct receptor subtypes. *J Pharmacol Exp Ther* **309:**758–768.

Goldman LA, Cutrone EC, Kotenko SV, Krause CD, and Langer JA (1996) Modifications of vectors pEF-BOS, pcDNA1 and pcDNA3 result in improved convenience and expression. *Biotechniques* **21:**1013–1015.

Hale JJ, Lynch CL, Neway W, Mills SG, Hajdu R, Keohane CA, Rosenbach MJ, Milligan JA, Shei GJ, Parent SA, et al. (2004a) A rational utilization of high-throughput screening affords selective, orally bioavailable 1-benzyl-3-carboxyazetidine sphingosine-1-phosphate-1 receptor agonists. *J Med Chem* **47:**6662–6665.

Hale JJ, Yan L, Neway WE, Hajdu R, Bergstrom JD, Milligan JA, Shei GJ, Chrebet GL, Thornton RA, Card D, et al. (2004b) Synthesis, stereochemical determination and biochemical characterization of the enantiomeric phosphate esters of the novel immunosuppressive agent FTY720. *Bioorg Med Chem* **12:**4803–4807.

Halgren TA (1996) Merck molecular force field. I. Basis, form, scope, parameterization, and performance of MMFF94. *J Comput Chem* **17:**490–519.

Holst B, Holliday ND, Bach A, Elling CE, Cox HM, and Schwartz TW (2004) Common structural basis for constitutive activity of the ghrelin receptor family. *J Biol Chem* **279:**53806–53817.

Inagaki Y, Pham TT, Fujiwara Y, Kohno T, Osborne DA, Igarashi Y, Tigyi G, and Parrill AL (2005) Sphingosine 1-phosphate analogue recognition and selectivity at S1P4 within the endothelial differentiation gene family of receptors. *Biochem J* **389:**187–195.

Jo E, Sanna MG, Gonzalez-Cabrera PJ, Thangada S, Tigyi G, Osborne DA, Hla T, Parrill AL, and Rosen H (2005) S1P1-selective in vivo-active agonists from high-throughput screening: off-the-shelf chemical probes of receptor interactions, signaling, and fate. *Chem Biol* **12:**703–715.

Kiuchi M, Adachi K, Kohara T, Minoguchi M, Hanano T, Aoki Y, Mishina T, Arita M, Nakao N, Ohtsuki M, et al. (2000) Synthesis and immunosuppressive activity of 2-substituted 2-aminopropane-1,3-diols and 2-aminoethanols. *J Med Chem* **43:**2946–2961.

Kohno T and Igarashi Y (2003) Truncation of the N-terminal ectodomain has implications in the N-glycosylation and transport to the cell surface of Edg-1/S1P1 receptor. *J Biochem (Tokyo)* **134:**667–673.

Kohno T, Wada A, and Igarashi Y (2002) N-Glycans of sphingosine 1-phosphate receptor Edg-1 regulate ligand-induced receptor internalization. *FASEB J* **16:**983–992.

Li Z, Chen W, Hale JJ, Lynch CL, Mills SG, Hajdu R, Keohane CA, Rosenbach MJ, Milligan JA, Shei GJ, et al. (2005) Discovery of potent 3,5-diphenyl-1,2,4-oxadiazole sphingosine-1-phosphate-1 (S1P1) receptor agonists with exceptional selectivity against S1P2 and S1P3. *J Med Chem* **48:**6169–6173.

Mandala S, Hajdu R, Bergstrom J, Quackenbush E, Xie J, Milligan J, Thornton R, Shei GJ, Card D, Keohane C, et al. (2002) Alteration of lymphocyte trafficking by sphingosine-1-phosphate receptor agonists. *Science (Wash DC)* **296:**346–349.

Meng EC and Bourne HR (2001) Receptor activation: what does the rhodopsin structure tell us. *Trends Pharmacol Sci* **22:**587–593.

Miller MD, Sheridan RP, and Kearsley SK (1999) SQ: a program for rapidly producing pharmacophorically relevent [sic] molecular superpositions. *J Med Chem* **42:**1505–1514.

Nakamichi H and Okada T (2006a) Crystallographic analysis of primary visual photochemistry. *Angew Chem Int Ed Engl* **45:**4270–4273.

Nakamichi H and Okada T (2006b) Local peptide movement in the photoreaction intermediate of rhodopsin. *Proc Natl Acad Sci USA* **103:**12729–12734.

Okada T, Fujiyoshi Y, Silow M, Navarro J, Landau EM, and Shichida Y (2002) Functional role of internal water molecules in rhodopsin revealed by X-ray crystallography. *Proc Natl Acad Sci USA* **99:**5982–5987.

Okada T, Sugihara M, Bondar AN, Elstner M, Entel P, and Buss V (2004) The retinal conformation and its environment in rhodopsin in light of a new 2.2 Å crystal structure. *J Mol Biol* **342:**571–583.

Palczewski K, Kumasaka T, Hori T, Behnke CA, Motoshima H, Fox BA, Le Trong I, Teller DC, Okada T, Stenkamp RE, et al. (2000) Crystal structure of rhodopsin: a G protein-coupled receptor. *Science (Wash DC)* **289:**739–745.

Parrill AL, Wang D, Bautista DL, Van Brocklyn JR, Lorincz Z, Fischer DJ, Baker DL, Liliom K, Spiegel S, and Tigyi G (2000) Identification of Edg1 receptor residues that recognize sphingosine 1-phosphate. *J Biol Chem* **275:**39379–39384.

Pyne S and Pyne N (2000) Sphingosine 1-phosphate signalling via the endothelial differentiation gene family of G-protein-coupled receptors. *Pharmacol Ther* **88:**115–131.

Renzetti AR, Catalioto RM, Criscuoli M, Cucchi P, Ferrer C, Giolitti A, Guelfi M, Rotondaro L, Warner FJ, and Maggi CA (1999) Relevance of aromatic residues in transmembrane segments V to VII for binding of peptide and nonpeptide antagonists to the human tachykinin NK_2 receptor. *J Pharmacol Exp Ther* **290:**487–495.

Salom D, Lodowski DT, Stenkamp RE, Le Trong I, Golczak M, Jastrzebska B, Harris T, Ballesteros JA, and Palczewski K (2006) Crystal structure of a photoactivated deprotonated intermediate of rhodopsin. *Proc Natl Acad Sci USA* **103:**16123–16128.

Sanna MG, Liao J, Jo E, Alfonso C, Ahn MY, Peterson MS, Webb B, Lefebvre S, Chun J, Gray N, et al. (2004) Sphingosine 1-phosphate (S1P) receptor subtypes S1P1 and S1P3, respectively, regulate lymphocyte recirculation and heart rate. *J Biol Chem* **279:**13839–13848.

Shin N, Coates E, Murgolo NJ, Morse KL, Bayne M, Strader CD, and Monsma FJ Jr (2002) Molecular modeling and site-specific mutagenesis of the histamine-binding site of the histamine H4 receptor. *Mol Pharmacol* **62:**38–47.

Spalding TA, Burstein ES, Henderson SC, Ducote KR, and Brann MR (1998) Identification of a ligand-dependent switch within a muscarinic receptor. *J Biol Chem* **273:**21563–21568.

Spiegel S and Milstien S (2003) Sphingosine-1-phosphate: an enigmatic signalling lipid. *Nat Rev Mol Cell Biol* **4:**397–407.

Tawadrous MN, Mabuchi A, Zimmermann A, and Wheatley AM (2002) Effects of immunosuppressant FTY720 on renal and hepatic hemodynamics in the rat. *Transplantation* **74:**602–610.

Teller DC, Okada T, Behnke CA, Palczewski K, and Stenkamp RE (2001) Advances in determination of a high-resolution three-dimensional structure of rhodopsin, a model of G-protein-coupled receptors (GPCRs). *Biochemistry* **40:**7761–7772.

Thompson JD, Higgins DG, and Gibson TJ (1994) CLUSTAL W: improving the sensitivity of progressive multiple sequence alignment through sequence weighting, position-specific gap penalties and weight matrix choice. *Nucleic Acids Res* **22:**4673–4680.

van Rhee AM and Jacobson KA (1996) Molecular architecture of G protein-coupled receptors. *Drug Dev Res* **37:**1–38.

Wang DA, Lorincz Z, Bautista DL, Liliom K, Tigyi G, and Parrill AL (2001) A single amino acid determines lysophospholipid specificity of the S1P1 (EDG1) and LPA1 (EDG2) phospholipid growth factor receptors. *J Biol Chem* **276:**49213–49220.

Xie JH, Nomura N, Koprak SL, Quackenbush EJ, Forrest MJ, and Rosen H (2003) Sphingosine-1-phosphate receptor agonism impairs the efficiency of the local immune response by altering trafficking of naive and antigen-activated CD4+ T cells. *J Immunol* **170:**3662–3670.

Address correspondence to: Dr. Stephen A. Parent, Merck Research Laboratories, PO Box 2000, RY80Y-225, Rahway, NJ 07065. E-mail: steve_parent@merck.com